Polarization-dependent infrared reflectivity study of $Sr_{2.5}Ca_{11.5}Cu_{24}O_{41}$ under pressure: Charge dynamics, charge distribution, and anisotropy

S. Frank,[1] A. Huber,[1] U. Ammerahl,[2] M. Hücker,[3] and C. A. Kuntscher[1,*]

[1]*Experimentalphysik 2, Universität Augsburg, D-86195 Augsburg, Germany*

[2]*Laboratoire de Physico-Chimie de LÉtat Solide, ICMMO, UMR 8182, Université Paris-Sud, 91405 Orsay, Cedex, France*

[3]*Condensed Matter Physics and Materials Science Department, Brookhaven National Laboratory, Upton, New York 11973, USA*

(Received 3 November 2014; revised manuscript received 27 November 2014; published 18 December 2014)

We present a polarization-dependent infrared reflectivity study of the spin-ladder compound $Sr_{2.5}Ca_{11.5}Cu_{24}O_{41}$ under pressure. The optical response is strongly anisotropic, with the highest reflectivity along the ladders/chains ($\mathbf{E}\|c$) revealing a metallic character. For the polarization direction perpendicular to the ladder plane, an insulating behavior is observed. With increasing pressure the optical conductivity for $\mathbf{E}\|c$ shows a strong increase, which is most pronounced below 2000 cm^{-1}. According to the spectral weight analysis of the $\mathbf{E}\|c$ optical conductivity the hole concentration in the ladders increases with increasing pressure and tends to saturate at high pressure. At ~7.5 GPa the number of holes per Cu atom in the ladders has increased by $\Delta\delta = 0.09(\pm 0.01)$, and the Cu valence in the ladders has reached the value +2.33. The optical data suggest that $Sr_{2.5}Ca_{11.5}Cu_{24}O_{41}$ remains electronically highly anisotropic up to high pressure, also at low temperatures.

DOI: 10.1103/PhysRevB.90.224516 PACS number(s): 78.20.−e, 78.30.−j, 62.50.−p, 71.45.Lr

I. INTRODUCTION

The quasi-one-dimensional spin ladder compounds $Sr_{14-x}Ca_xCu_{24}O_{41}$ have been studied extensively due to the emergence of superconductivity for high Ca content and high pressure [1–6]. The theoretically [1] predicted superconducting state was first observed in $Sr_{0.4}Ca_{13.6}Cu_{24}O_{41.84}$ below $T_c = 12$ K and for pressures $\geqslant 3$ GPa [5]. The crystal structure of $Sr_{14-x}Ca_xCu_{24}O_{41}$ consists of two types of copper oxide layers that are parallel to the crystallographic *a*–*c* plane and alternate along the *b* axis: the Cu_2O_3 planes which contain the two-leg ladders, and CuO_2 planes containing chains with edge-shared CuO_4 plaquettes [2]. At ambient conditions the parent compound $Sr_{14}Cu_{24}O_{41}$ has an intrinsic hole doping of six holes per formula unit, which results in an average Cu valence of +2.25. Although the substitution of Sr by isovalent Ca does not change the intrinsic charge concentration in the system, the physical properties alter drastically, which has been attributed to a redistribution of hole carriers among the ladder and chain subsystems [2].

Among the key issues for understanding the mechanism of superconductivity in $Sr_{14-x}Ca_xCu_{24}O_{41}$ are the distribution of charge carriers among the ladders and chains, and the dimensionality of the system. Both aspects can be addressed by polarization-dependent infrared spectroscopy, which is also applied in the present study. According to optical studies for the undoped parent compound $Sr_{14}Cu_{24}O_{41}$, at ambient conditions one hole resides on the ladders and five holes on the chains [7]. These values are close to those found by XAS and NMR experiments [8–11]. Ca doping changes the carrier distribution as was recently discussed and summarized in Ref. [10]: despite some discrepancies in the absolute number of holes, it is now generally accepted that Ca doping triggers a chemical pressure induced transfer of holes from the chains to the ladders.

Besides a high Ca content, high pressure is needed to induce superconductivity in $Sr_{14-x}Ca_xCu_{24}O_{41}$ [5,12]. The pressure-dependent charge distribution in $Sr_{14-x}Ca_xCu_{24}O_{41}$ has been studied by NMR measurements for $x = 0$ and $x = 12$ for pressures up to 3.2 GPa. According to this study the hole concentration on the ladders increases by $\Delta\delta \approx 0.03$ per Cu atom in $Sr_2Ca_{12}Cu_{24}O_{41}$, when a pressure of 3.2 GPa is applied. Furthermore, pressure-dependent electrical transport measurements on $Sr_{2.5}Ca_{11.5}Cu_{24}O_{41}$ suggest that the superconducting state has a quasi-two-dimensional character [13].

In the present study we investigate the charge distribution in $Sr_{2.5}Ca_{11.5}Cu_{24}O_{41}$ up to a pressure of 7.5 GPa by infrared spectroscopy. Additionally, we address the dimensionality of the system under pressure by presenting polarization-dependent infrared spectra at room temperature and at low temperature.

II. EXPERIMENT

The studied $Sr_{2.5}Ca_{11.5}Cu_{24}O_{41}$ single crystal was grown by the traveling-solvent floating zone technique [14]. The polarization-dependent room-temperature reflectivity as a function of pressure was measured over a broad frequency range (300–12000 cm^{-1}) using a Bruker IFS 66v/S Fourier transform infrared spectrometer. Two diamond-anvil pressure cells were employed for pressure generation: a clamp diamond-anvil cell (Diacell cryoDAC-Mega) and a Syassen-Holzapfel diamond-anvil cell (DAC) [15]. Finely ground CsI powder served as quasihydrostatic pressure transmitting medium to ensure direct contact of the sample with the diamond anvil. The sample size was $80 \times 80\ \mu m^2$ for the high-frequency range and about $200 \times 200\ \mu m^2$ for frequencies below 700 cm^{-1} to avoid diffraction effects. To focus the infrared beam onto the small sample in the pressure cell, a Bruker IR Scope II infrared microscope with a 15× magnification objective was used. Spectra taken at the inner diamond-air interface of the empty DAC served as the reference for normalization of the sample spectra (see Ref. [16] for an illustration of the measurement geometry). The absolute reflectivity at the sample-diamond interface, denoted as $R_{s\text{-}d}$, was calculated according to $R_{s\text{-}d}(\omega) = R_{\mathrm{dia}} \times I_s(\omega)/I_d(\omega)$, where $I_s(\omega)$

*christine.kuntscher@physik.uni-augsburg.de

denotes the intensity spectrum reflected from the sample-diamond interface and $I_d(\omega)$ the reference spectrum of the diamond-air interface. For R_{dia} a value of 0.167 was calculated from the refractive index of diamond n_{dia}, which is assumed to be independent of pressure.

The polarization-dependent reflectivity measurements for frequencies 780–6000 cm^{-1} at low temperature and high pressure were carried out using a home-built infrared microscope coupled to the FTIR spectrometer and maintained at the same vacuum conditions, in order to avoid absorption lines of H_2O and CO_2 molecules. Details about the home-built infrared microscope can be found in Ref. [17]. A Syassen-Holzapfel DAC [15] for the pressure generation was mounted in a continuous-flow helium cryostat (Cryo Vac KONTI cryostat). More details about the geometry of the reflectivity measurements can be found in our earlier publications [18,19]. As reference, we used the intensity reflected from the silver coated steel gasket inside the DAC. Correspondingly, the absolute reflectivity at the sample-diamond interface $R_{s\text{-}d}$ was calculated according to $R_{s\text{-}d}(\omega) = I_s(\omega)/I_{Ag}(\omega)$, where $I_s(\omega)$ denotes the intensity spectrum reflected from the sample-diamond interface and $I_{Ag}(\omega)$ the reference spectrum of the diamond-silver interface. All reflectivity spectra shown in this paper refer to the absolute reflectivity at the sample-diamond interface $R_{s\text{-}d}$. The pressure in the DAC was determined *in situ* by the standard ruby-fluorescence technique [20].

III. RESULTS AND ANALYSIS

The pressure-dependent reflectivity spectra of $Sr_{2.5}Ca_{11.5}Cu_{24}O_{41}$ at room temperature are depicted in Figs. 1(a)–1(c) for the polarization direction along the ladders/chains ($\mathbf{E}\|c$), along the rungs ($\mathbf{E}\|a$), and perpendicular to the ladder plane ($\mathbf{E}\|b$), respectively. Features in the frequency range 1700–2700 cm^{-1} are artifacts originating from multiphonon absorptions in the diamond anvils, which are not fully corrected by the normalization procedure, and are not considered in the following analysis of the spectra. The polarization-dependent reflectivity spectra at the lowest applied pressure clearly reveal the electronic anisotropy of $Sr_{2.5}Ca_{11.5}Cu_{24}O_{41}$, consistent with earlier results [7,21,22]: for $\mathbf{E}\|c$, i.e., along the ladders and chains, the overall

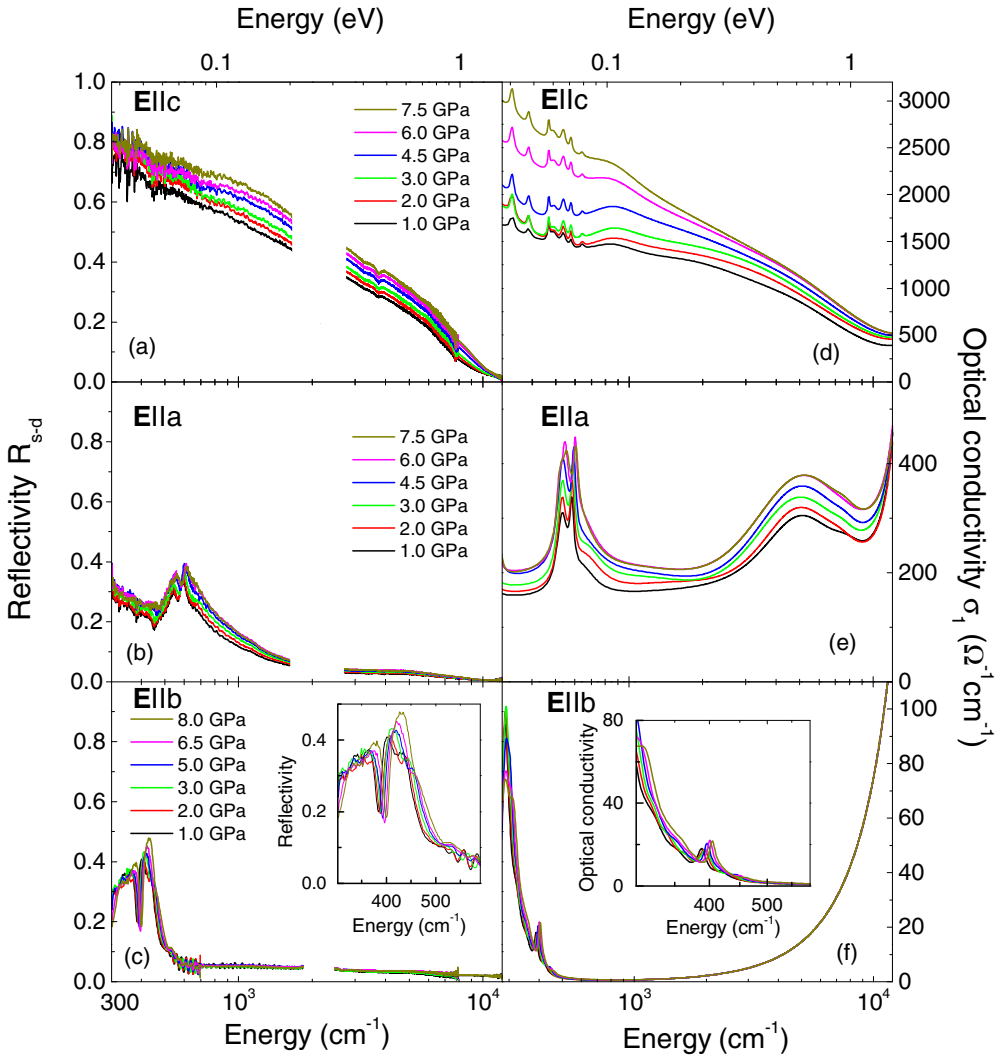

FIG. 1. (Color online) (a)–(c) Reflectivity spectra $R_{s\text{-}d}$ of $Sr_{2.5}Ca_{11.5}Cu_{24}O_{41}$ for the polarization $\mathbf{E}$ of the radiation along the three crystal axes at room temperature. (d)–(f) Real part of the optical conductivity σ_1 obtained from the Drude-Lorentz fitting of the reflectivity spectra.

reflectivity is high, whereas for $\mathbf{E}\|a$ it is considerably lower, but still reveals a metallic behavior (see also the corresponding optical conductivity as described below). For $\mathbf{E}\|b$ a typical insulating behavior is found, with an overall low reflectivity and strong phonon excitations in the low-frequency range. As compared to the results from ambient-pressure measurements on $Sr_{2.5}Ca_{11.5}Cu_{24}O_{41}$ the observed phonon modes have a lower intensity and are broadened. According to the pressure-dependent reflectivity data the electronic anistropy of the sample is preserved up to the highest applied pressure (≈8 GPa): for $\mathbf{E}\|c$ the reflectivity increases monotonically with increasing pressure. Also for $\mathbf{E}\|a$ a gradual albeit weaker increase is found. Along the insulating $\mathbf{E}\|b$ direction the reflectivity does not change with pressure, except the alterations related to the phonon excitations.

The real part of the optical conductivity σ_1 was obtained by fitting the reflectivity spectra with the Drude-Lorentz model [23] combined with the normal-incidence Fresnel equation

$$R_{s\text{-}d} = \left|\frac{n_{\mathrm{dia}} - \sqrt{\epsilon_s}}{n_{\mathrm{dia}} + \sqrt{\epsilon_s}}\right|^2, \quad \epsilon_s = \epsilon_\infty + \frac{i\sigma}{\epsilon_0\omega}, \qquad (1)$$

where n_{dia} is the refractive index of diamond and ϵ_s the complex dielectric function of the sample. ϵ_∞ is the optical dielectric constant. The so-obtained optical conductivity spectra are shown in Figs. 1(d)–1(f) for the three polarization directions. The optical conductivity is highest for $\mathbf{E}\|c$ and the metallic character is clearly revealed by a Drude contribution. The various contributions to the optical conductivity are illustrated in Fig. 2: besides the Drude term a pronounced midinfrared absorption band (MIR band) centered at around 2000 cm^{-1} and phonon excitations are found. For $\mathbf{E}\|a$ the conductivity at the lowest frequencies is finite indicating a metallic character. At around 5000 cm^{-1} an absorption band is observed followed by the onset of higher-frequency excitations. For $\mathbf{E}\|b$ the low-energy optical conductivity contains phonon excitations

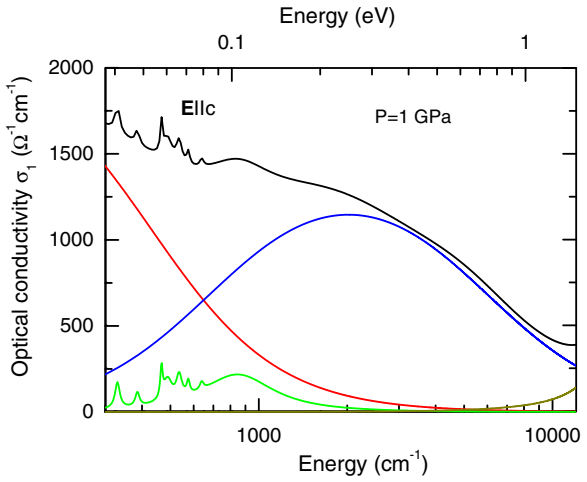

FIG. 2. (Color online) Real part of the optical conductivity σ_1 for $\mathbf{E}\|c$ at the lowest applied pressure at room temperature and the various contributions (Drude term, MIR band, and phonon modes) as obtained from the Drude-Lorentz fits.

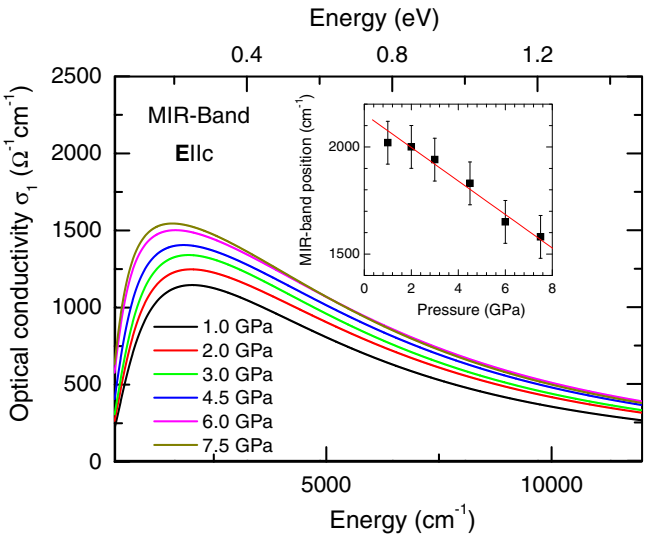

FIG. 3. (Color online) MIR band as a function of pressure at room temperature, as obtained from the Drude-Lorentz fits of the reflectivity spectra. Inset: position of the MIR band as a function of pressure.

besides higher-frequency excitations with the main spectral weight above the measured frequency range.

With increasing pressure a strong increase in the $\mathbf{E}\|c$ optical conductivity is observed, which is most pronounced below 2000 cm^{-1} [see Fig. 1(d)]. Based on the Drude-Lorentz fit of the pressure-dependent reflectivity spectra, the MIR band was extracted and is depicted in Fig. 3. From the maxima we have estimated the energy position of the MIR band, which we plot in the inset of Fig. 3 as a function of pressure. One can see that with increasing pressure the MIR band shows a redshift. Simultaneously, its spectral weight increases. For the polarization $\mathbf{E}\|a$ the overall optical conductivity increases with increasing pressure [see Fig. 1(e)]. The frequencies of the phonon modes were obtained from the Drude-Lorentz fits and are depicted in Fig. 4(a). The phonon modes show a slight hardening with increasing pressure. The mode at 530 cm^{-1} splits into two modes above 4.5 GPa. For $\mathbf{E}\|b$ the overall optical conductivity is pressure independent, except for the low-frequency range, where the phonon modes are observed [see Fig. 1(f) and its inset]. The pressure dependence of the phonon frequencies from the Drude-Lorentz fits are plotted in Fig. 4(b). The phonon modes harden with increasing pressure. Above 2 GPa additional, but weak phonon modes appear, and above 4.5 GPa the phonon mode close to 400 cm^{-1} splits. In general, a pressure-induced symmetry change of the crystal structure will modify the phonon spectrum—with typical signatures being anomalies in the pressure-induced frequency shifts, mode intensity or width, or splitting of modes. In the case of $Sr_{2.5}Ca_{11.5}Cu_{24}O_{41}$ the new high pressure modes appear as shoulders of the strong modes observed at ambient conditions. These additional modes might already be present at ambient conditions and their intensity just increases upon pressure application due to charge redistribution, such as a transfer of charges from the chains to the ladders; therefore, we hesitate to interpret them in terms of pressure-induced crystal symmetry changes. Also the nonhydrostatic components of

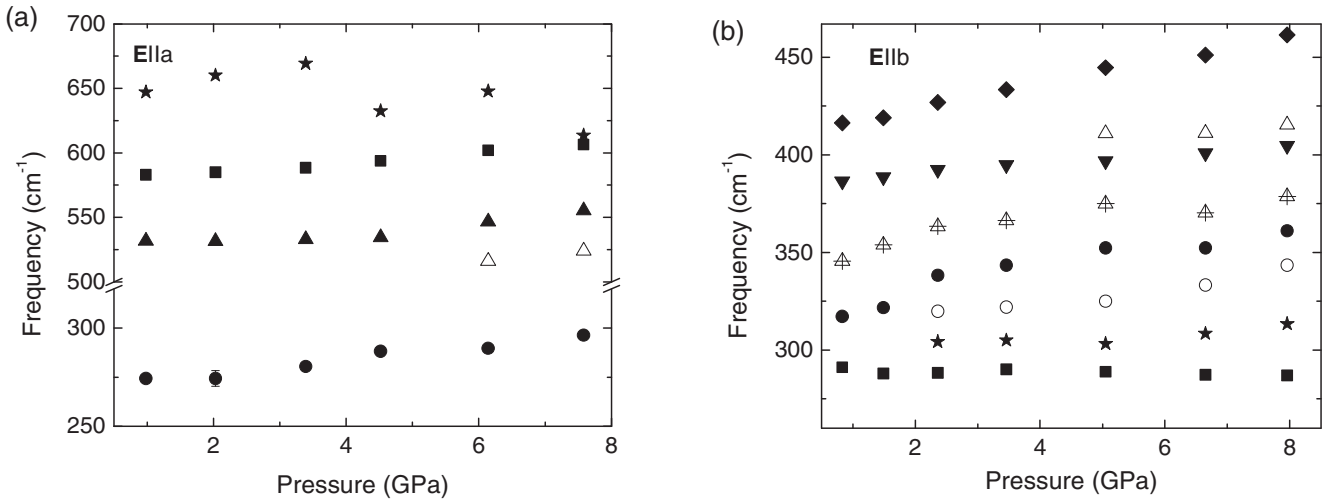

FIG. 4. Frequencies of the phonon modes as a function of pressure at room temperature, as obtained from the Drude-Lorentz fits of the reflectivity spectra, for (a) $\mathbf{E}\|a$ and (b) $\mathbf{E}\|b$.

the pressure in the DAC might play a role. Furthermore, it is difficult to attribute the observed phonon modes to Cu-O vibrations of either chains or ladders, since the bond lengths are similar. In conclusion, the pressure dependence of the infrared-active phonon modes support the findings of x-ray diffraction measurements, which did not find indications for a pressure-induced structural phase transition up to 9 GPa [24,25].

Additional information on the pressure dependence of the electronic properties of $Sr_{2.5}Ca_{11.5}Cu_{24}O_{41}$ has been obtained by reflectivity measurements within the ladder plane for higher pressures, i.e., up to 15 GPa (see Fig. 5). Along both $\mathbf{E}\|c$ and $\mathbf{E}\|a$ directions the reflectivity spectra barely change for pressures above ∼9 GPa. All above-described changes with pressure are reversible upon pressure release.

IV. DISCUSSION

A. Pressure-induced hole transfer onto the ladders

The high conductivity in $Sr_{14-x}Ca_xCu_{24}O_{41}$ along the c direction has been attributed to the charge carriers of the ladder subunits [7,26,27]. Optical studies of $Sr_{14}Cu_{24}O_{41}$ at ambient conditions found an intrinsic hole doping of six holes per formula unit, with one hole in the Cu_2O_3 ladders and five holes in the CuO_2 chains at ambient conditions [7]. This distribution of holes among ladders and chains is close to the one found by XAS and NMR experiments [8–10]. With increasing Ca doping the total carrier concentration in the material is conserved, but the physical properties change drastically, which was attributed to a redistribution of charge carriers from the chains to the ladders with increasing Ca content [2,7,9,26–34]. Because the ionic radius of Ca is smaller than that of Sr, the lattice parameter b decreases for increasing Ca content [35]. Since a similar effect occurs when external pressure is applied [24,25], the substitution of Sr by Ca can be interpreted in terms of a chemical pressure. Thus one may ask whether the application of external pressure causes a similar charge carrier redistribution.

The real part of the optical conductivity of $Sr_{2.5}Ca_{11.5}Cu_{24}O_{41}$ for $\mathbf{E}\|c$ (see Fig. 2) consists of a Drude term and an MIR band. Upon pressure application an increase in the optical conductivity is observed, which is most pronounced for the frequency range below about 2000 cm^{-1}. Obviously, this increase suggests a redistribution of spectral weight from high to low frequencies. According to the sum rule (see below) the spectral weight is a measure of the effective charge carrier concentration N_{eff}. The excitations below

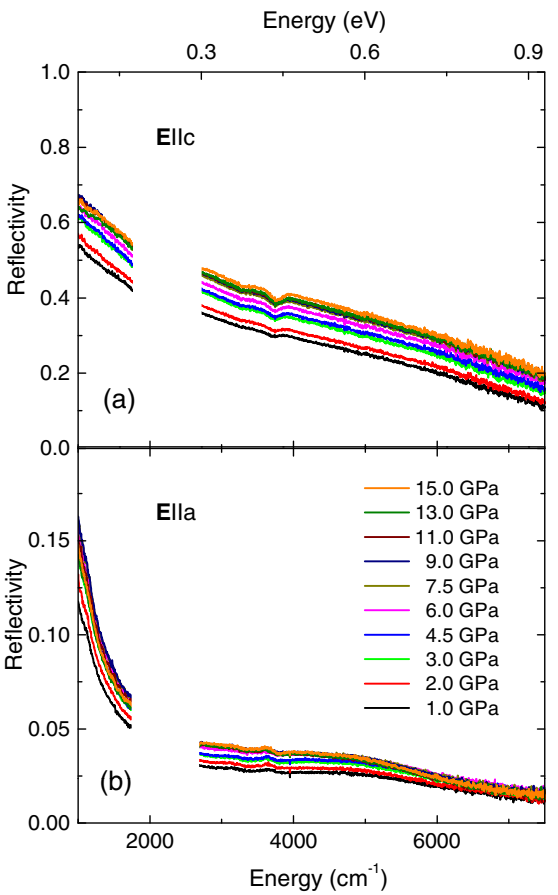

FIG. 5. (Color online) Reflectivity spectra of $Sr_{2.5}Ca_{11.5}Cu_{24}O_{41}$ for (a) $\mathbf{E}\|c$ and (b) $\mathbf{E}\|a$ up to 15 GPa at room temperature.

1.2 eV (≈9678 cm^{-1}) can be attributed to the ladders, whereas those above 1.2 eV are related to the chains [7]. Therefore, the increase in the low-frequency optical conductivity is related to a transfer of holes from the chain to the ladder subsystem.

By applying the sum rule the number of charge carriers in the ladders can be calculated from the optical conductivity spectrum according to

$$N_{\mathrm{eff}}(\omega_2) = \frac{2m^*V}{\pi e^2}\int_{\omega_1}^{\omega_2}\sigma_1(\omega')d\omega', \qquad (2)$$

where m^* is the effective mass of the charge carriers, V the pressure-dependent volume of the unit cell, and $\omega_1 = 300\ cm^{-1}$, i.e., the lowest measured frequency. Hereby, we assume that only the holes on the ladder subunits are mobile, i.e., the spectral weight for the conducting $\mathbf{E}\|c$ direction in the frequency range up to $\omega_2 = 1.2$ eV is related to the holes of the ladders [7,36]. Hence the calculated N_{eff} gives the effective carrier concentration in the ladders per Cu atom δ according to $N_{\mathrm{eff}} = A\delta$, where A is a constant determined according to literature data (see details given below).

To be able to calculate the effective charge carrier concentration N_{eff} the pressure-dependent volume of the unit cell must be known. Since corresponding data are not available for the studied compound, we made use of the linear pressure coefficients for the lattice parameters of the closely related compound $Sr_{0.4}Ca_{13.6}Cu_{24}O_{41}$ [24,25] for which values of $\alpha = 0{,}0093$ Å/GPa, $\beta = 0{,}0823$ Å/GPa, and $\gamma = 0{,}0074$ Å/GPa, respectively, can be found in the literature [37]. These values were applied to the lattice parameters of $Sr_{2.5}Ca_{11.5}Cu_{24}O_{41}$. The so-obtained volume of the unit cell is depicted in Fig. 6.

To obtain the effective carrier concentration in the ladders per Cu atom, δ, from the spectral weight according to $N_{\mathrm{eff}} = A\delta$, the coefficient A needs to be determined. This parameter was obtained based on published results for $Sr_{14}Cu_{24}O_{41}$, for which NEXAFS and optical measurements found one hole per formula unit on the ladders [7,13]. With 14 Cu atoms on the ladder units per unit cell, this gives $\delta = \frac{1}{14} = 0.07$ (corresponding ladder Cu valence of +2.07). From the spectral weight analysis of the optical data of Osafune *et al.* [7] we obtain $N_{\mathrm{eff}} \approx 0.148$, which gives $A = \frac{N_{\mathrm{eff}}}{\delta} = 2.12$.

For a consistency check, the above-described procedure has been applied to our lowest-pressure data of $Sr_{2.5}Ca_{11.5}Cu_{24}O_{41}$, which should deviate only slightly from the ambient-pressure data. We find $V = 549{,}26$ $Å^3$ and the spectral weight $8.93 \times 10^6\ \Omega^{-1}cm^{-2}$ at $\omega_2 = 1.2$ eV, which gives $N_{\mathrm{eff}}(\omega_2) = 0.523$ according to Eq. (2). From this value the number of holes in the ladders per Cu atom is calculated according to $\delta = \frac{N_{\mathrm{eff}}}{A} = 0.25 \pm 0.01$, corresponding to a ladder Cu valence of +2.25. This result is in agreement with Ca doping dependent infrared measurements [7], where for $Sr_3Ca_{11}Cu_{24}O_{41}$ a hole concentration of 0.2 holes per Cu atom on the ladders (corresponding ladder Cu valence: +2.20) was found, keeping in mind the slightly higher Ca content and the pressure offset of 1 GPa in our measurement.

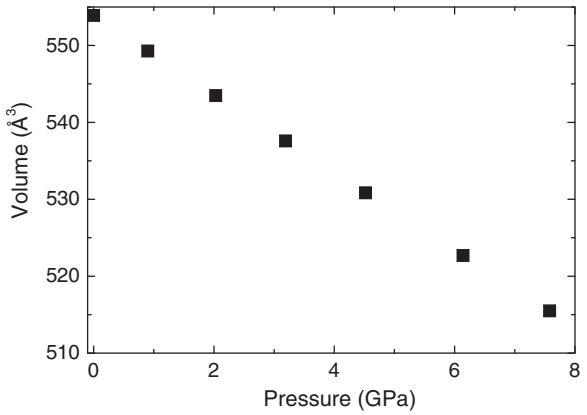

FIG. 6. Estimated unit cell volume of $Sr_{2.5}Ca_{11.5}Cu_{24}O_{41}$ as a function of pressure at room temperature.

The resulting effective charge concentration N_{eff} per Cu atom and the Cu valence of the ladder subunits as a function of applied pressure are depicted in Figs. 7(a) and 7(b). With increasing pressure the Cu valence and the related number of holes in the ladders increases and tends to saturate at high pressure. At $P \sim 7.5$ GPa the number of holes per Cu atom in the ladders has increased by 0.09 (±0.01) and the Cu valence in the ladders has reached the value +2.33 [see Fig. 7(b)]. Hence both Ca substitution and the application of external pressure lead to an increase of the charge carrier concentration on the ladders. Pressure-dependent NMR measurements on $Sr_2Ca_{12}Cu_{24}O_{41}$ observed a pressure-induced increase of $\Delta\delta \approx 0.03$ at ~3.2 GPa [9], which compares well with the value $\Delta\delta = 0.04 \pm 0.01$ at around 3 GPa according to our IR measurements [see inset of Fig. 7(b)].

Reflectivity spectra at higher pressures (>8 GPa) could only be obtained in the higher-frequency range (mid- and near-infrared) due to the diffraction limit and are plotted in Fig. 5. Obviously, the overall reflectivity increases with increasing pressure for both polarization directions $\mathbf{E}\|c$ and $\mathbf{E}\|a$ up to ~9 GPa and are basically constant above this pressure. From this behavior we infer that the spectral weight along the conducting c direction and the associated concentration of charge carriers on the ladders are approximately constant above ~9 GPa.

B. Nature of the MIR band

The optical conductivity spectrum of $Sr_{2.5}Ca_{11.5}Cu_{24}O_{41}$ for the polarization $\mathbf{E}\|c$ consists of a pronounced MIR band, whose origin will be discussed in the following based on its pressure dependence. Photoemission experiments at 130 K found an electronic band located at ~0.5 eV (4032 cm^{-1}) for $Sr_{14}Cu_{24}O_{41}$, which shifts toward the Fermi energy with increasing Ca content [38–40]. The band was interpreted in terms of strong electronic correlations. Within the single-band Hubbard model for correlated electron systems characteristic contributions are expected in the optical conductivity spectrum [41–44]. For the metallic solution of the Hubbard model a Drude term and an excitation band in the midinfrared frequency range are observed in the optical conductivity spectra, consistent with experimental findings [19,45–47]. These contributions are also present in the optical conductivity spectrum of $Sr_{2.5}Ca_{11.5}Cu_{24}O_{41}$ (see Fig. 2). With increasing pressure the MIR band shifts to smaller frequencies, which is consistent with a pressure-induced bandwidth increase. Although the spectral weight of the MIR band is large

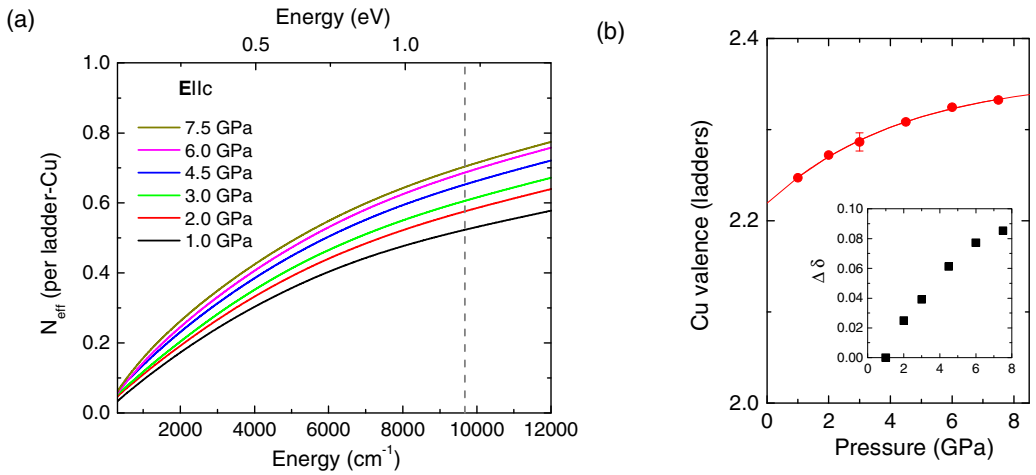

FIG. 7. (Color online) (a) Effective charge concentration N_{eff} per Cu atom obtained according to Eq. (2). (b) Cu valence in the ladders as a function of pressure. At high pressure the increase of holes in the ladders saturates. Inset: relative increase of the number of holes per Cu atoms in the ladders.

compared to that of the Drude term [44], an interpretation of the MIR band within the Hubbard model appears reasonable.

On the other hand, the importance of electron-phonon interaction in $Sr_{14-x}Ca_xCu_{24}O_{41}$ has been discussed earlier [38,48]. In fact, MIR absorption features are fingerprints for the excitation of polaronic quasiparticles. An interpretation of the MIR band in $Sr_{14-x}Ca_xCu_{24}O_{41}$ in terms of the dissociation of bipolarons composed of holes on one rung was suggested in Refs. [7,49]. Generally, polaronic excitations cause a characteristic MIR band in the optical conductivity spectrum, whose energy position is related to the polaron binding energy and which is expected to shift to lower frequencies with increasing pressure [16,50–53]. The pressure-induced shift of the MIR band in $Sr_{2.5}Ca_{11.5}Cu_{24}O_{41}$ to lower frequencies is thus consistent with the polaron picture.

Furthermore, it has been shown theoretically that in $Sr_{14-x}Ca_xCu_{24}O_{41}$ a pressure-induced phase transition from single polarons to bipolarons can occur [48]. During the formation of bipolarons two polarons are localized within the same potential well [50]. The absorption band of small bipolarons generally appears at higher energies compared to single small polarons, with the frequency position $\omega_p = 4E_b - U$, where E_b is the polaron binding energy and U the Coulomb interaction between the two polarons. Hence a pressure-induced phase transition of single polarons to bipolarons would result in a shift of the MIR band to higher frequencies. This is not observed in our data, and therefore such a phase transition seems to be unlikely.

C. Pressure-induced dimensional crossover?

In $Sr_{2.5}Ca_{11.5}Cu_{24}O_{41}$ superconductivity is observed at 4 GPa and 6 K [13]. Owing to the similarity in crystal structure with the high-temperature copper-oxide superconductors the question at issue is whether the superconductivity in $Sr_{14-x}Ca_xCu_{24}O_{41}$ is a one-dimensional or—like in the high-temperature superconductors—a two-dimensional phenomenon. It was suggested earlier that the superconductivity in the spin ladder compounds is of two-dimensional nature [9,13,54]. Pressure-dependent infrared data for various polarization directions can give insight into the anisotropy of a material [16,51,55].

According to Figs. 1(a)–1(c) only for the direction $\mathbf{E}\|c$ the reflectivity—and concomitant the optical conductivity—significantly increases under pressure. For illustration we plot in Fig. 8 the reflectivity level along the three polarization directions at 1000 cm^{-1}, i.e., outside the phonon mode region, which is representative for the overall behavior of the reflectivity spectra. For $\mathbf{E}\|b$ the reflectivity is unchanged under pressure, and for $\mathbf{E}\|a$ only a small increase of the reflectivity with increasing pressure is observed. Hence no strong increase of the reflectivity level for the directions perpendicular to $\mathbf{E}\|c$ is observed. Therefore, a pressure-induced dimensional crossover towards a more two-dimensional character at room temperature seems to be unlikely according to our data.

An electrical transport study suggested that pressurized $Sr_{2.5}Ca_{11.5}Cu_{24}O_{41}$ becomes two-dimensional at low temperature [13]. To test the dimensionality of the system within the ladder plane at low temperature, we carried out additional reflectivity measurements at various pressures. Figure 9 depicts the reflectivity spectra at 10 K for the polarization direction

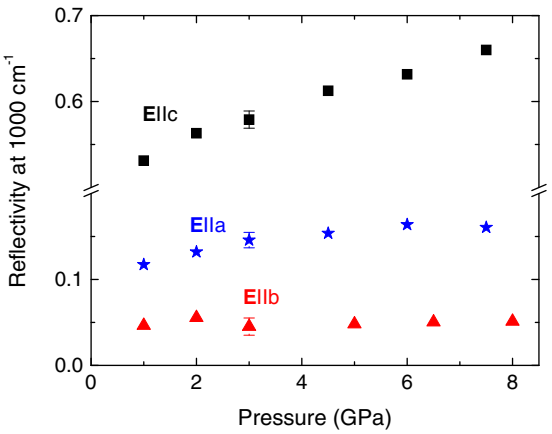

FIG. 8. (Color online) Room-temperature reflectivity of $Sr_{2.5}Ca_{11.5}Cu_{24}O_{41}$ at 1000 cm^{-1} for $\mathbf{E}\|c$, $\mathbf{E}\|a$, and $\mathbf{E}\|b$ as a function of pressure.

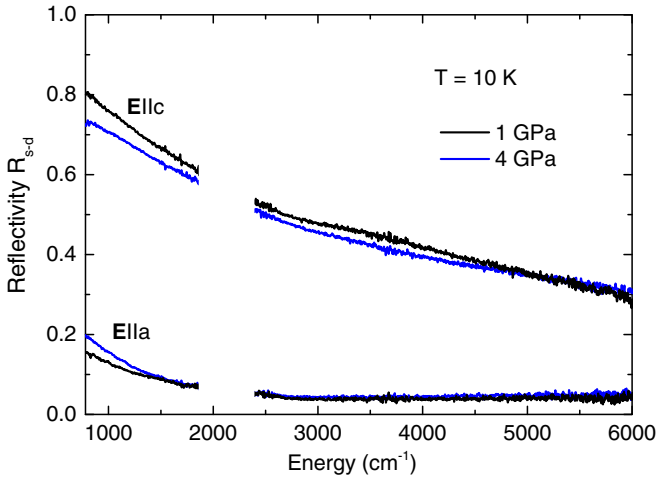

FIG. 9. (Color online) Reflectivity spectra $R_{s\text{-}d}$ of $Sr_{2.5}Ca_{11.5}Cu_{24}O_{41}$ at 10 K for the lowest (∼1 GPa) and highest (∼4 GPa) pressure for the two polarization directions $\mathbf{E}\|c$ and $\mathbf{E}\|a$ within the ladder/chain plane.

along the two crystal axes within the ladder/chain plane, i.e., along the c and a axis, at the lowest (∼1 GPa) and highest (∼4 GPa) applied pressure. Obviously, the anisotropy within the ladder/chain plane at base temperature is only slightly affected by pressure, and a crossover to two-dimensional electronic properties in $Sr_{2.5}Ca_{11.5}Cu_{24}O_{41}$ is not observed up to 4 GPa within the studied frequency range.

V. CONCLUSIONS

In conclusion, our polarization-dependent infrared reflectivity study shows that $Sr_{2.5}Ca_{11.5}Cu_{24}O_{41}$ is electronically highly anisotropic with a conducting behavior along the ladders and an insulating behavior perpendicular to the ladder plane. Along the ladder rungs the metallic character is lower as compared to the ladder direction. The pressure-induced increase in the reflectivity and the corresponding optical conductivity is strongest for the polarization direction along the ladders, $\mathbf{E}\|c$. The pronounced MIR band in the $\mathbf{E}\|c$ optical conductivity spectrum redshifts under pressure. The band can be attributed to strong electronic correlations or to the excitation of polaronic quasiparticles. The hole concentration in the ladders increases with increasing pressure and tends to saturate at high pressure, resulting in a Cu valence in the ladders of +2.33 at P∼7.5 GPa, which corresponds to an increase in the number of holes per ladder Cu atom by 0.09 (±0.01). Above 9 GPa the MIR reflectivity within the ladder plane is independent of pressure. $Sr_{2.5}Ca_{11.5}Cu_{24}O_{41}$ remains highly anisotropic up to high pressure and at low temperatures within the studied frequency range.

ACKNOWLEDGMENTS

This work is financially supported by the DFG (Grant No. KU1432/6-1). Work at Brookhaven was supported by the Office of Basic Energy Sciences (BES), Division of Materials Science and Engineering, U.S. Department of Energy (DOE), under Contract No. DE-AC02-98CH10886.

[1] E. Dagotto and T. M. Rice, Science **271**, 618 (1996).
[2] T. Vuletic, B. Korin-Hamzic, T. Ivek, S. Tomic, B. Gorshunov, M. Dressel, and J. Akimitsu, Phys. Rep. **428**, 169 (2006).
[3] B. J. Kim, H. Koh, E. Rotenberg, S.-J. Oh, H. Eisaki, N. Motoyama, S. Uchida, T. Tohyama, S. Maekawa, Z.-X. Shen *et al.*, Nat. Phys. **2**, 397 (2006).
[4] E. Dagotto, J. Riera, and D. Scalapino, Phys. Rev. B **45**, 5744(R) (1992).
[5] M. Uehara, T. Nagata, J. Akimitsu, H. Takahashi, N. Mori, and K. Kinoshita, J. Phys. Soc. Jpn. **65**, 2764 (1996).
[6] P. Abbamonte, G. Blumberg, A. Rusydi, A. Gozar, P. G. Evans, T. Siegrist, L. Venema, H. Eisaki, E. D. Isaacs, and G. A. Sawatzky, Nature (London) **431**, 1078 (2004).
[7] T. Osafune, N. Motoyama, H. Eisaki, and S. Uchida, Phys. Rev. Lett. **78**, 1980 (1997).
[8] N. Nücker, M. Merz, C. A. Kuntscher, S. Gerhold, S. Schuppler, R. Neudert, M. S. Golden, J. Fink, D. Schild, S. Stadler, V. Chakarian, J. Freeland, Y. U. Idzerda, K. Conder, M. Uehara, T. Nagata, J. Goto, J. Akimitsu, N. Motoyama, H. Eisaki, S. Uchida, U. Ammerahl, and A. Revcolevschi, Phys. Rev. B **62**, 14384 (2000).
[9] Y. Piskunov, D. Jerome, P. Auban-Senzier, P. Wzietek, and A. Yakubovsky, Phys. Rev. B **72**, 064512 (2005).
[10] M.-J. Huang, G. Deng, Y. Y. Chin, Z. Hu, J.-G. Cheng, F. C. Chou, K. Conder, J.-S. Zhou, T.-W. Pi, J. B. Goodenough, H.-J. Lin, and C. T. Chen, Phys. Rev. B **88**, 014520 (2013).
[11] Please note that the values obtained by the recent XAS study by Rusydi *et al.* [31] differ largely from other XAS results.
[12] N. Motoyama, H. Eisaki, S. Uchida, N. Takeshita, N. Mori, T. Nakanishi, and H. Takahashi, Europhys. Lett. **58**, 758 (2002).
[13] T. Nagata, M. Uehara, J. Goto, J. Akimitsu, N. Motoyama, H. Eisaki, S. Uchida, H. Takahashi, T. Nakanishi, and N. Mori, Phys. Rev. Lett. **81**, 1090 (1998).
[14] U. Ammerahl and A. Revcolevschi, J. Cryst. Growth **197**, 825 (1999).
[15] R. Keller and W. B. Holzapfel, Rev. Sci. Instrum. **48**, 517 (1977); G. Huber, K. Syassen, and W. B. Holzapfel, Phys. Rev. B **15**, 5123 (1977).
[16] S. Frank, C. A. Kuntscher, I. Loa, K. Syassen, and F. Lichtenberg, Phys. Rev. B **74**, 054105 (2006).
[17] C. A. Kuntscher, A. Huber, and M. Hücker, Phys. Rev. B **89**, 134510 (2014).
[18] A. Pashkin, M. Dressel, and C. A. Kuntscher, Phys. Rev. B **74**, 165118 (2006).
[19] C. A. Kuntscher, S. Frank, A. Pashkin, M. Hoinkis, M. Klemm, M. Sing, S. Horn, and R. Claessen, Phys. Rev. B **74**, 184402 (2006).
[20] H. K. Mao, J. Xu, and P. M. Bell, J. Geophys. Res. **91**, 4673 (1986).
[21] T. Osafune, N. Motoyama, H. Eisaki, S. Uchida, and S. Tajima, Phys. Rev. Lett. **82**, 1313 (1999).
[22] B. Ruzicka, L. Degiorgi, U. Ammerahl, G. Dhalenne, and A. Revcolevschi, Eur. Phys. J. B **6**, 301 (1998).

[23] F. Wooten, *Optical Properties of Solids* (Academic, New York, 1972).
[24] M. Isobe, T. Ohta, M. Onoda, F. Izumi, S. Nakano, J. Q. Li, Y. Matsui, E. Takayama-Muromachi, T. Matsumoto, and H. Hayakawa, Phys. Rev. B **57**, 613 (1998).
[25] S. Pachot, P. Bordet, R. J. Cava, C. Chaillout, C. Darie, M. Hanfland, M. Marezio, and H. Takagi, Phys. Rev. B **59**, 12048 (1999).
[26] N. Motoyama, T. Osafune, T. Kakeshita, H. Eisaki, and S. Uchida, Phys. Rev. B **55**, R3386(R) (1997).
[27] T. F. A. Müller, V. Anisimov, T. M. Rice, I. Dasgupta, and T. Saha-Dasgupta, Phys. Rev. B **57**, R12655 (1998).
[28] S. A. Carter, B. Batlogg, R. J. Cava, J. J. Krajewski, W. F. Peck, Jr., and T. M. Rice, Phys. Rev. Lett. **77**, 1378 (1996).
[29] E. Tafra, B. Korin-Hamzic, M. Basletic, A. Hamzic, M. Dressel, and J. Akimitsu, Phys. Rev. B **78**, 155122 (2008).
[30] K. Magishi, S. Matsumoto, Y. Kitaoka, K. Ishida, K. Asayama, M. Uehara, T. Nagata, and J. Akimitsu, Phys. Rev. B **57**, 11533 (1998).
[31] A. Rusydi, M. Berciu, P. Abbamonte, S. Smadici, H. Eisaki, Y. Fujimaki, S. Uchida, M. Rübhausen, and G. A. Sawatzky, Phys. Rev. B **75**, 104510 (2007).
[32] E. Kabasawa, J. Nakamura, N. Yamada, K. Kuroki, H. Yamazaki, M. Watanabe, J. D. Denlinger, S. Shin, and R. C. C. Perera, J. Phys. Soc. Jpn. **77**, 034704 (2008).
[33] G. Deng, V. Pomjakushin, V. Petricek, E. Pomjakushina, M. Kenzelmann, and K. Conder, Phys. Rev. B **84**, 144111 (2011).
[34] V. Ilakovac, C. Gougoussis, M. Calandra, N. B. Brookes, V. Bisogni, S. G. Chiuzbaian, J. Akimitsu, O. Milat, S. Tomić, and C. F. Hague, Phys. Rev. B **85**, 075108 (2012).
[35] E. M. McCarron, M. A. Subramanian, J. C. Calabrese, and R. L. Harlow, Mater. Res. Bull. **23**, 1355 (1988).
[36] The excitations of the holes in the chains are observed for frequencies larger than ∼2.5 eV [7], which is well above the measured frequency range.
[37] The linear pressure coefficient α (β, γ) was obtained from the pressure dependence of the lattice parameter a (b, c) by a linear fit to the experimental data according to the equation $a(P) = a(0) + \alpha P$, where $a(P)$ is the lattice parameter a at a pressure P.
[38] T. Takahashi, T. Yokoya, A. Ashihara, O. Akaki, H. Fujisawa, A. Chainani, M. Uehara, T. Nagata, J. Akimitsu, and H. Tsunetsugu, Phys. Rev. B **56**, 7870 (1997).
[39] T. Sato, T. Yokoya, T. Takahashi, M. Uehara, T. Nagata, J. Goto, and J. Akimitsu, J. Phys. Chem. Solids **59**, 1912 (1998).
[40] T. Yokoya, H.-D. Kim, A. Ashihara, H. Kumigashira, H. Fujisawa, T. Takahashi, M. Uehara, T. Nagata, and J. Akimitsu, Physica C **282–287**, 997 (1997).
[41] M. J. Rozenberg, G. Kotliar, and H. H. Kajueter, Phys. Rev. B **54**, 8452 (1996).
[42] M. J. Rozenberg, G. Kotliar, H. Kajueter, G. A. Thomas, D. H. Rapkine, J. M. Honig, and P. Metcalf, Phys. Rev. Lett. **75**, 105 (1995).
[43] M. Imada, A. Fujimori, and Y. Tokura, Rev. Mod. Phys. **70**, 1039 (1998).
[44] M. Jarrell, J. K. Freericks, and T. Pruschke, Phys. Rev. B **51**, 11704 (1995).
[45] I. Kezsmarki, N. Hanasaki, D. Hashimoto, S. Iguchi, Y. Taguchi, S. Miyasaka, and Y. Tokura, Phys. Rev. Lett. **93**, 266401 (2004).
[46] I. Kezsmarki, N. Hanasaki, K. Watanabe, S. Iguchi, Y. Taguchi, S. Miyasaka, and Y. Tokura, Phys. Rev. B **73**, 125122 (2006).
[47] C. A. Kuntscher, A. Pashkin, H. Hoffmann, S. Frank, M. Klemm, S. Horn, A. Schönleber, S. van Smaalen, M. Hanfland, S. Glawion, M. Sing, and R. Claessen, Phys. Rev. B **78**, 035106 (2008).
[48] E. Kaneshita, I. Martin, and A. R. Bishop, Phys. Rev. B **73**, 094514 (2006).
[49] C. A. Hayward, D. Poilblanc, and D. J. Scalapino, Phys. Rev. B **53**, R8863 (1996).
[50] D. Emin, Phys. Rev. B **48**, 13691 (1993).
[51] C. A. Kuntscher, S. Frank, I. Loa, K. Syassen, T. Yamauchi, and Y. Ueda, Phys. Rev. B **71**, 220502(R) (2005).
[52] K. Thirunavukkuarasu, F. Lichtenberg, and C. A. Kuntscher, J. Phys.: Condens. Matter **18**, 9173 (2006).
[53] J. Ebad-Allah, L. Baldassarre, M. Sing, R. Claessen, V. A. M. Brabers, and C. A. Kuntscher, J. Phys.: Condens. Matter **25**, 035602 (2013).
[54] T. Vuletic, B. Korin-Hamzic, S. Tomic, B. Gorshunov, P. Haas, T. Room, M. Dressel, J. Akimitsu, T. Sasaki, and T. Nagata, Phys. Rev. Lett. **90**, 257002 (2003).
[55] A. Pashkin, M. Dressel, M. Hanfland, and C. A. Kuntscher, Phys. Rev. B **81**, 125109 (2010).